Solid-Particles Flow Regimes in Air/Water Stratified Flow in a Horizontal Pipeline

Ramin Dabirian, Ram S. Mohan, and **Ovadia Shoham,** The University of Tulsa, and **Gene Kouba,** Chevron (retired)

Summary

The entrainment of solid particles in crude oil occurs during production from reservoirs with low formation strength. The stationary solid-particles bed at the horizontal pipe bottom can cause operational problems such as production decline, excessive pressure loss, equipment failure, erosion, and corrosion. Solid-particles deposition can be managed by operating above the critical solid-particles-deposition velocity, which is the velocity that maintains the continuous movement of particles at the pipe bottom. Here, a comprehensive analysis of solid-particle flow regimes in stratified flow in a horizontal pipeline is presented, which is a novel contribution because it is applied to multiphase flow. The effect of concentration on the solid-particle flow regimes and identification of the critical solid-particles-deposition velocities for various particle concentrations are also investigated.

The understanding of solid-particle flow regimes in pipelines for any given set of operational conditions is important for identifying the nature of particle interaction and movement. Experimental studies are conducted in a 4-in. horizontal pipeline for a stratified flow regime that uses air, water, and glass beads at relatively low solid-particles concentrations (<10,000 ppm). The effects of different experimental conditions, such as gas velocity, solid-particles concentration, and particle size, are investigated in this study. Six main solid-particles flow regimes in horizontal air/water flow are identified, and can be distinguished visually: fully dispersed solid flow, dilute solids at wall, concentrated solids at wall, moving dunes, stationary dunes, and stationary bed. Therefore, the critical solid-particles-deposition velocities are determined on the basis of the transition between moving (concentrated solids at wall/moving dunes, as appropriate) and stationary (stationary dunes/bed, as appropriate) solid particles. The experimental data show that with small particle size, the critical solid-particles-deposition velocity is almost independent of concentration, while with larger particle sizes, the critical velocity increases with the concentration.

Introduction

Most oil and gas reservoirs have unconsolidated formations with low formation strength, and, hence, are prone to producing sand. New wells usually produce high fractions of sand in the cleanup stage. Over time the sand production stabilizes to a low level before reaching the end of reservoir life, which increases again because of pore-pressure reduction, which supports some of the weight of the overlying rock. Solid-particles deposition can decrese the production rate of a reservoir as a result of accumulation in the wellbore or in the pipeline, and can also cause excessive costs for operation of upstream facilities.

In the oil and gas industry, sand production impacts the asset integrity of production systems. Erosion from high flow rates can cause severe damage to upstream facilities such as pipelines, fittings, chokes, separators, and other control equipment. Furthermore, failure of the facilities because of erosion results in shutting down of the entire production over a period of time. Thus, solid-particles transport is inevitably a problem in the petroleum industry.

There are a few studies covering solid-particles transport in multiphase pipelines. Solid-particles transport is complicated because it depends on several variables, including flow patterns, fluid properties, phase velocities, and pipe-geometry features such as roughness, diameter, and inclination angle. Each of these variables can have significant effects on the solid-particles-transport process.

More attention has been paid recently to the importance of tracking solid-particles-transport management over reservoir life. There are three options available for managing solid-particles transport: applying a cleaning operation, installing solid-particles exclusion facilities, and operating above the critical solid-particles-deposition velocity. Cleaning operations, such as pigging, are only applicable for small amounts of solid particles, and they often result in the pig becoming stuck if the pigging frequency is not high enough. Installing solid-particles exclusion systems (e.g., gravel packs) can reduce production and create excessive pressure drops. The third option, operating above the critical solid-particles-deposition velocity, is preferred for solid-particles-production management as a prevention technique under favorable operating conditions because it has practical applications and can be beneficial commercially.

To avoid solid-particles deposition, it is necessary to manage solid-particles transport above solid-particles-deposition velocities. On the other hand, operating under unnecessarily high flow rates is not only cost inefficient, but can also create facility damages; therefore, it is necessary to find the optimum velocity to maintain continuous particle movement. This velocity is called the critical solid-particles-deposition velocity.

Solid-Particles Flow Regimes

Particle interactions and movement have a significant effect on transport of solid particles. Shamlou (1987) defined the most common classification for solid-particles transport in horizontal pipeline as homogeneous flow, heterogeneous flow, heterogeneous and sliding flow, saltation flow, and stationary bed. Doron and Barnea (1996) and Ibarra et al. (2016) defined three main solid-particles flow regimes as suspension, moving bed, and stationary bed. The suspension solid-particles flow regime was further divided into two subpatterns of pseudohomogeneous suspension and heterogeneous suspension.

Well-defined flow regimes will clarify under what conditions the particles are moving more or less independently (i.e., not locked together as in a sliding bed). Flow regimes in this paper are applied to multiphase flow, whereas Doron and Barnea (1996) and other flow-regime publications are applicable for single-phase flow only. According to this study, there are six main solid-particles flow regimes in stratified flow in a multiphase pipeline: fully dispersed solid flow, dilute solids at the wall, concentrated solids at the wall, moving dunes, stationary dunes, and stationary bed. Each one is described in the following subsections and shown in **Fig. 1.**

Fully Dispersed Solids Flow. At high flow rates, there is a suspension of particles in which particles are completely dispersed in the liquid phase, with no particles touching the pipe bottom.

Dilute Solids at the Wall. At slightly lower flow rates, some particles drag along the pipe bottom and start rolling on the pipe. In this solid-particles flow regime, no particle interactions are observed at the pipe bottom, hence particle shape is not important.
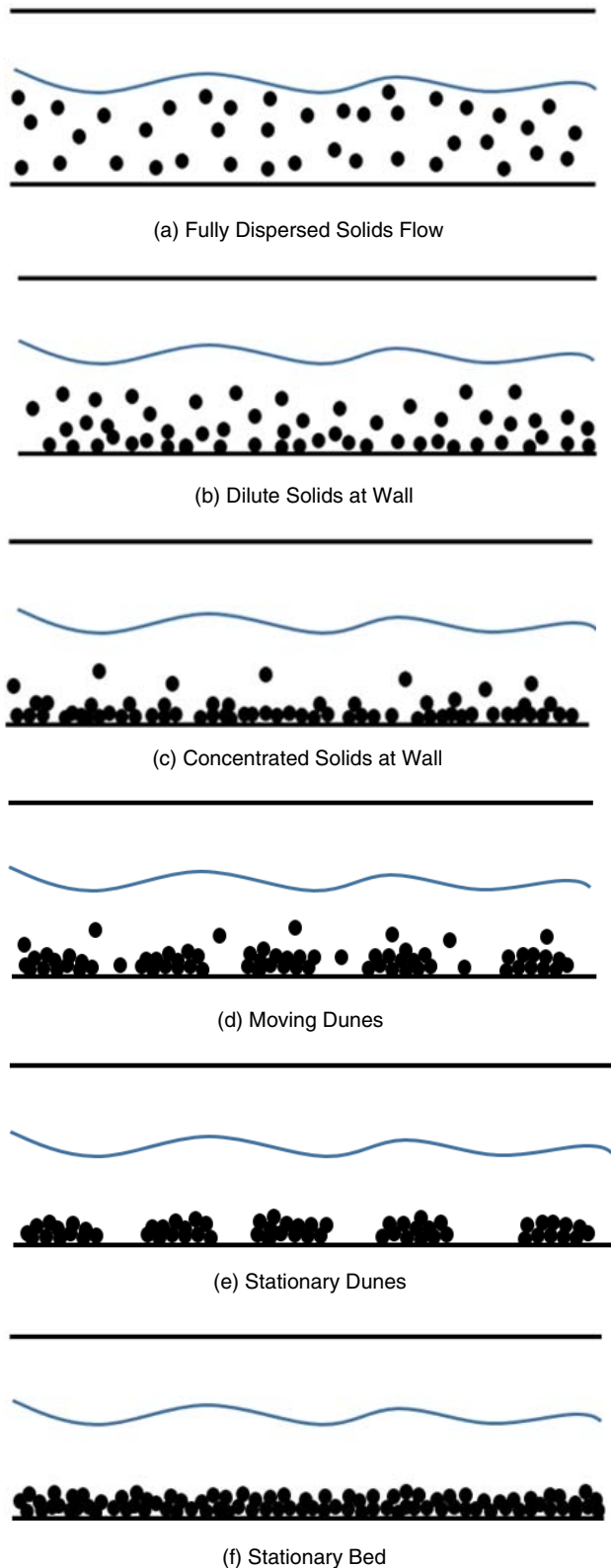
(a) Fully Dispersed Solids Flow

(b) Dilute Solids at Wall

(c) Concentrated Solids at Wall

(d) Moving Dunes

(e) Stationary Dunes

(f) Stationary Bed

Fig. 1—2D view of solid-particles flow regime in stratified flow (Dabirian et al. 2015).

Concentrated Solids at the Wall. With further decreasing flow rates, higher solid-particles concentrations are created on the wall, and there are high particle interactions. A particle is moved because it is pushed by other particles rather than by rolling itself. Hence, particle shape is important for this flow regime.

Moving Dunes. At slower flow rates, the turbulence created by waves at the gas/liquid interface scatters the top of the moving bed, and a discontinuously moving bed is generated at the pipe bottom. In this regime, the clusters of particles come together and start creeping discontinuously at the pipe bottom. Moving dunes are observed at very low concentrations or at air/liquid/solid flow with small particle sizes.

Stationary Dunes. At low flow rates, the dunes stop moving, and stationary dunes are observed. This solid-particles flow regime is seen near the 2D and 3D wave transition at the interface. For stationary dunes, we have lesser microbial interaction (compared with stationary bed) between the solid particle and pipeline, leading to reduced corrosion.

Stationary Bed. At considerably low flow rates, solid particles start to deposit and remain at rest, and stationary particles are observed at the pipe bottom.

Critical Velocity
The transition between solid-particles flow regimes is characterized by a critical velocity. Critical-velocity values depend on the type of solid-particles flow regime and are usually related to solid-particles deposition and solid-particles suspension. Critical solid-particles-deposition velocity is defined as the velocity required to deposit a solid particle that is initially moving in the liquid phase at the pipe bottom, while suspension critical velocity is the velocity required to pick up and suspend a solid particle that is initially at rest. The difference between these two velocities can be caused by additional cohesive force, when the solid-particles bed is created at the pipe bottom. Salama (1999) defined critical suspending velocity as the transition between solid-particles suspension and solid-particles moving bed. According to Salama (1999), the critical suspending velocity is the minimum velocity to suspend solid particles in liquid phase and to prevent excessive pipe erosion. Many terms have been defined by authors for the upper limit of a stationary bed. Shook and Roco (1991) applied the term "deposition velocity," while Wood (1979) used the term "deposit velocity." Wilson (1976) and Doron and Barnea (1996) also used the term "limit deposit velocity." According to Ibarra et al. (2016), the critical sand-deposition velocity is defined as the minimum velocity needed to keep all particles moving along the pipe, which is determined as the transition between moving bed and stationary bed. Similarly, in the current study, the critical solid-particles-deposition velocity is defined as the minimum velocity that keeps the particles moving continuously. However, it is determined on the basis of the transition between moving (concentrated solids at wall/moving dunes, as appropriate) and stationary (stationary dunes/bed, as appropriate) sand particles.

Experimental Program
A unique facility was designed and constructed with a horizontal 4-in. transparent polyvinyl chloride (PVC) pipe, which measures liquid velocity, liquid holdup, and pressure drop (Nguyen et al. 2014). The designed test loop uses water as its liquid phase and air as its gas phase, along with glass beads with spherical shape representing the solid particles. The particle-diameter range is between 45 and 600 μm (in three different groups) with an average density of 2475 kg/m^3, which was selected to ensure thorough mixing and separation performance.

As seen in **Fig. 2,** the solid-particles water slurry is prepared in a 100-gal tank with a conical bottom, which is equipped with two electronic batch mixers with 1,750-rev/min capacity. Each mixer includes three stainless-steel propellers to ensure a homogeneous slurry in the tank. A 6-in. baffle is installed in the tank to prevent vortexing and aeration created by the mixers. A recirculation line, which injects the slurry into the bottom of the tank, is used to create a more homogeneous slurry. The outlet line of the mixing tank is connected to a centrifugal pump. The pump, which is used to flow the slurry to the test section is equipped with a 2-hp electric motor. The slurry-flow rate is controlled by a manual valve located downstream of the centrifugal pump. An electromagnetic flowmeter is used to measure slurry-flow rate with
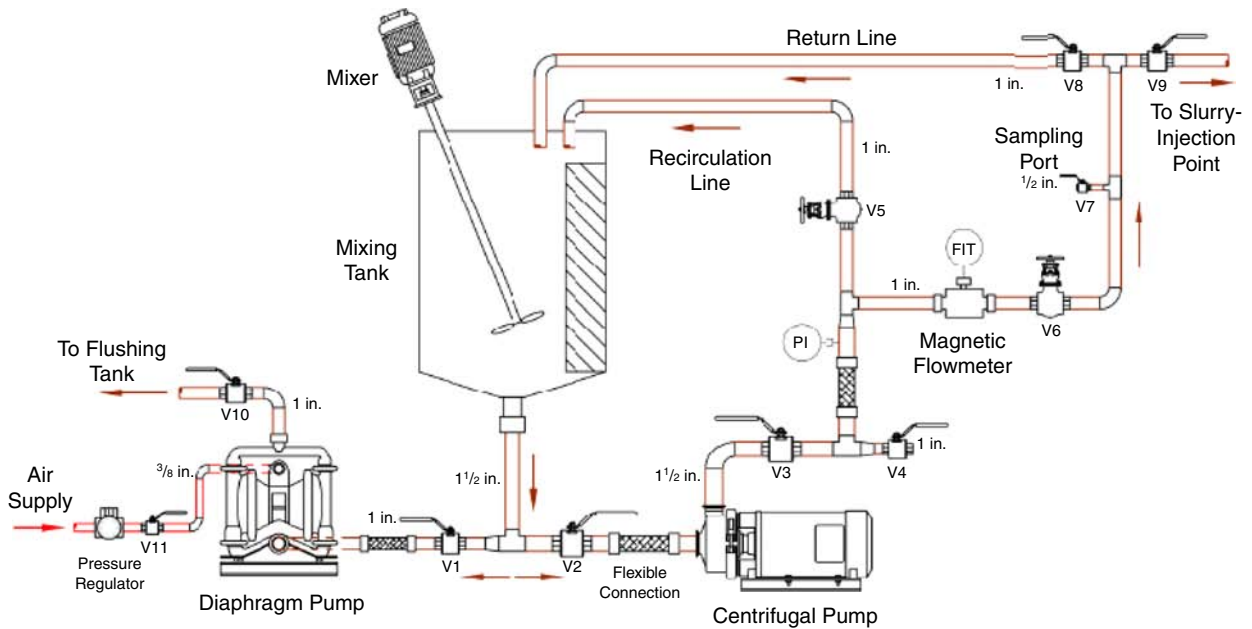
Fig. 2—Schematic of the slurry section (Ibarra et al. 2016).

high accuracy. The flowmeter was calibrated by flowing slurry with different sand concentrations from the tank passing through the flowmeter. The initial and final slurry volume in the tank, as well as the flowing time, are recorded for calculating the volumetric flow rate, which is compared with the instrument reading. The tank outlet line is connected to a diaphragm pump—with a flow-rate capacity of 35 gal/min and particle-size capacity of 3175 μm—which is powered by compressed air.

The air is provided by a 60-hp electric compressor with a maximum flow-rate capacity of 1,200 scf/min and maximum operating pressure of 120 psig. To measure the air-flow rate, a Coriolis mass flowmeter is used, which has a maximum flow-rate capacity of 1,000 lbm/min. A pneumatic valve is used to control the air-flow rate automatically. **Fig. 3** presents the schematic of the flow loop in plan view, where all the pipes are oriented horizontally.
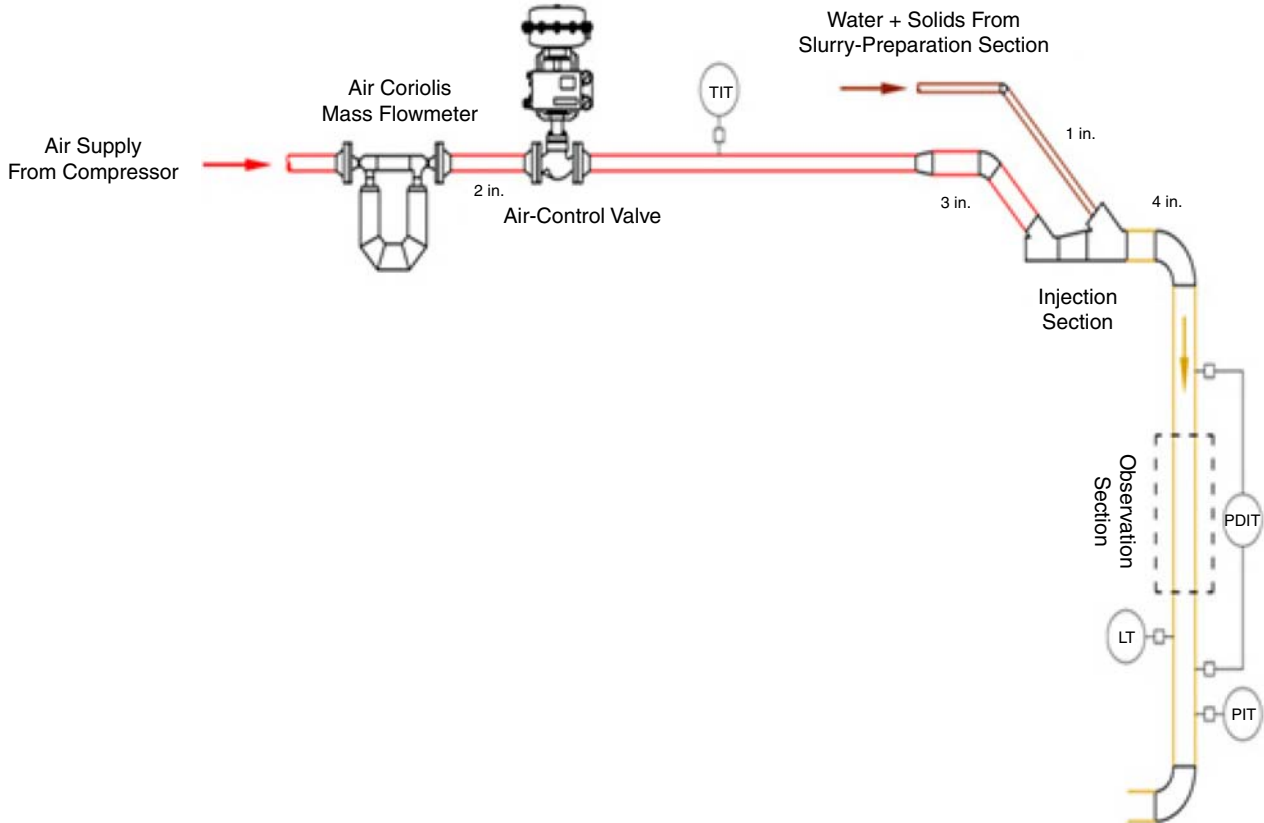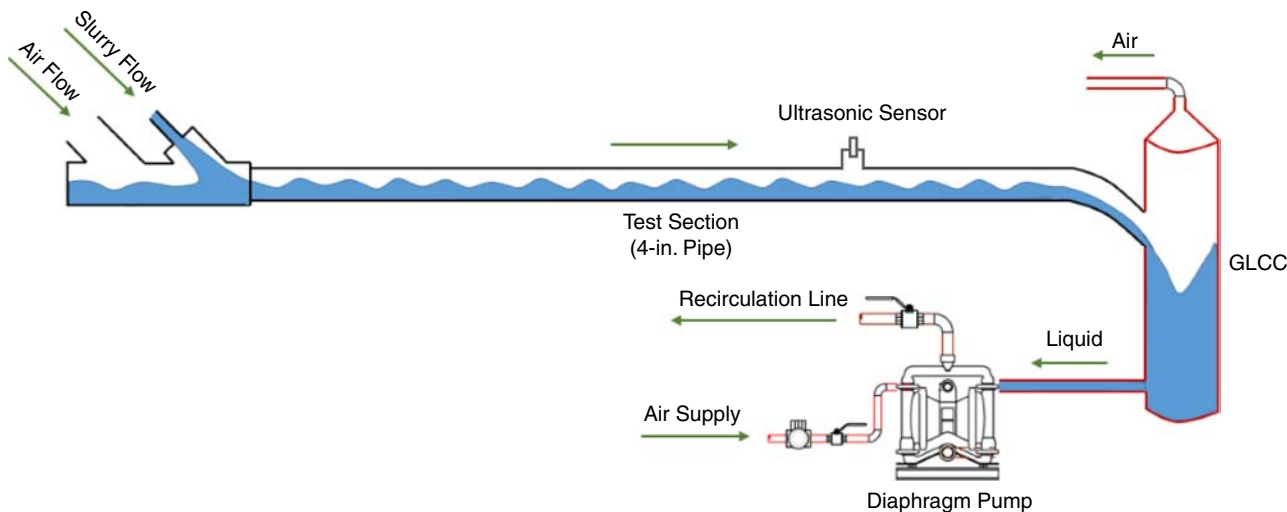

Fig. 3—Schematic of the flow loop.

Fig. 4—Schematic of the test section.

Fig. 4 shows the upstream of the test section, which is a 4-in. Schedule-80 PVC pipe measuring 11 m in length. The mixture of air and slurry is injected at the upstream of the test section. The air and slurry are injected from a 45° angle from the top of the pipe to create smooth mixing and to avoid high turbulence and unexpected slugs. The test section is equipped with an ultrasonic proximity sensor with a sensing range between 100 and 600 mm to measure the liquid level in the center of the 4-in. pipe. At the downstream of the test section, a gas/liquid cylindrical-cyclone (GLCC) separator is used to separate the air from the slurry. The flow entering the GLCC creates a swirling motion, which causes the two-phase flow of gas and liquid to separate by centrifugal force. The liquid is pushed toward the wall of the separator, and is removed from the bottom, while the gas (lighter phase) is forced toward the center of the separator, and is removed from the top. The air is released to the atmosphere, and the slurry is recirculated continuously into the slurry tank.

The experimental conditions have been selected to ensure that the particles are transported in the 4-in. pipe in a stratified flow regime because it is most prone to sand deposition compared with other flow regimes, owing to the low liquid velocity and lack of mixing. The effects of different experimental conditions, such as differing gas velocity, solid-particles concentration, and particle size, have been investigated in this study. To ensure stratified flow, superficial liquid velocities of 0.05, 0.1, and 0.12 m/s and superficial gas velocities ranging from 2.5 to 14 m/s have been selected. The particle sizes are selected to ensure homogeneous mixing in the slurry tank and to ensure high particle suspension in the test section. **Table 1** presents the detailed test matrix of this study.
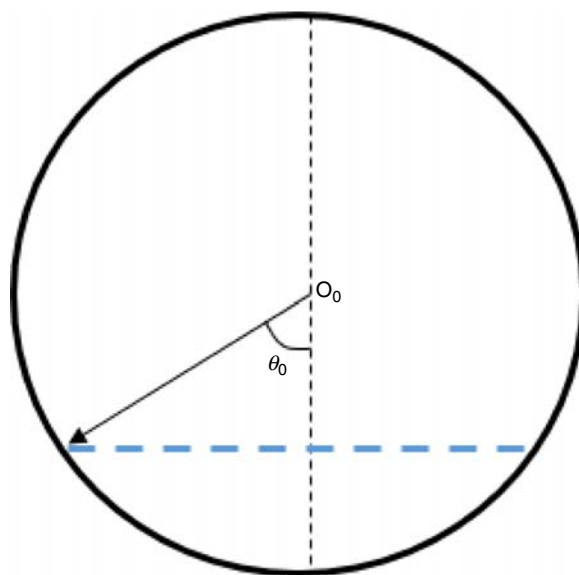
Test Procedure. The first step is to prepare the slurry of solid particles and water at specific concentrations in the slurry tank. The flow rates of air and slurry are selected to ensure gas/liquid strat-ified flow in the pipe and to enable the observation of different solid-particles flow regimes at the pipe bottom. At the specified superficial liquid velocity, the superficial gas velocity is reduced step by step to observe different solid-particles flow regimes and also to find the transition to critical solid-particles-deposition velocity. During the experiment, liquid levels and gas- and liquid-flow rates are measured to calculate the superficial and actual liquid and gas velocities, and also the liquid holdup.

Liquid Holdup. An ultrasonic sensor installed at the top of the pipe (Fig. 4) measures the liquid height in the center of the pipe. If the liquid-holdup calculation is based on the liquid height alone, it will not be accurate. To improve the accuracy of the liquid-holdup calculation, the double-circle model, as proposed by Yongqian (2005), is applied here. The model consists of two circles, the inner pipe wall circle and an imaginary eccentric circle. The gas/liquid interface is represented by the imaginary circle. When the diameter of the imaginary circle is very large, the gas/liquid interface approaches a flat configuration, and the imaginary circle is not considered (**Fig. 5**), and otherwise, the interface has a concave configuration.

Variable	Range
Pipe inner diameter (in.)	3.78
Particle specific gravity	2.475
Particle size (µm)	45–90, 125–250, and 425–600
Solid-particles concentration (ppm)	100–10,000
Superficial gas velocity, V_{SG} (m/s)	2.5–14
Superficial liquid velocity, V_{SL} (m/s)	0.05, 0.1, and 0.12

Table 1—Experimental test matrix.

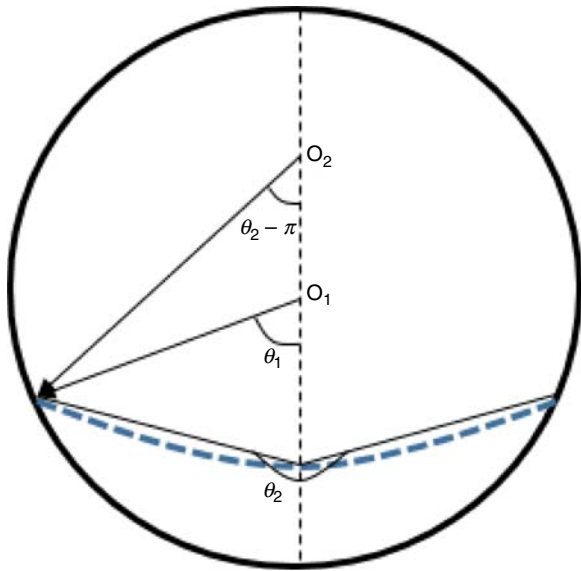**Fig. 5—Gas/liquid interface with flat configuration.**

Fig. 6—Gas/liquid interface with concave configuration.

For the case of the flat gas/liquid interface, the relationship between the central angle θ_o (radians) and the liquid holdup H_L can be written as

$$H_L = \frac{1}{\pi}\left[\theta_o - \frac{1}{2}\sin(2\theta_o)\right]. \quad\text{.....................................(1)}$$

When the gas/liquid interface has a concave shape (Fig. 6), the relationship between H_L, θ_1, and θ_2 is calculated by

$$H_L = \frac{1}{\pi}\left\{\theta_1 - \frac{1}{2}\sin(2\theta_1) - \frac{\sin^2\theta_1}{\sin^2\theta_2}\left[\theta_2 - \pi - \frac{1}{2}\sin(2\theta_2)\right]\right\}. \quad\text{....(2)}$$

By measuring the liquid height at the center and side of pipe, liquid holdup can be measured easily on the basis of the double-

circle model given by Eqs. 1 and 2. Brauner et al. (1996) and Yongqian (2005) may be referred to for more details.

Experimental Result. The flow conditions of all experimental runs are plotted on a Taitel and Dukler (1976) flow-pattern map predicted for 4-in. pipe (**Fig. 7**). For all runs, a stratified wavy flow regime is observed. Because the maximum sand concentration in terms of particle mass fraction is less than 1%, it is believed that the existence of the particles will not have any significant effect on the flow regime.

Flow-Regime Sequences. Solid-particles transport in gas/liquid two-phase flow is complicated because it depends on various parameters such as particle geometry, particle concentration, and fluid properties. Among the parameters, particle size plays an important role in creating different solid-particles flow regimes. Preliminary experiments were conducted to identify various flow regimes that exist in gas/liquid solid-particles flow. To investigate solid-particles flow-regime sequences, the superficial liquid velocity is kept constant, and superficial gas velocity is reduced step by step to visualize the solid-particles flow regimes. The solid-particles flow sequences for three particle sizes of 45–90, 125–250, and 425–600 µm are separately described in detail next.

Particle Size: 45–90 µm. At high gas velocities, the solid particles are fully suspended in the liquid phase, and the turbulence created by the liquid phase and gas/liquid interface is high enough to pick up particles from the pipe bottom and keep them dispersed in the liquid phase. **Fig. 8** shows the bottom view of the pipe with the 45- to 90-µm particles.

With decreasing gas velocity, the first solid-particles streaks are seen on the pipe sides instead of the pipe center. This phenomenon occurs at high gas velocity when a 3D wave is observed at the gas/liquid interface, and the interface has a crescent shape. At these flow conditions, the liquid height at the pipe center is lower compared with that at the pipe sides. Consequently, the particles can be picked up and suspended easily in the center compared with at the pipe sides. The higher the liquid height, the more difficult it becomes to keep particles suspended.

At lower gas velocities, there is still a 3D wave at the interface, but the interface has a concave shape. At these flow conditions, more streaks, which move parallel to each other, are seen at the bottom of the liquid cross-sectional area. In a turbulent flow, there are counter-rotating longitudinal vortices, in which the au-
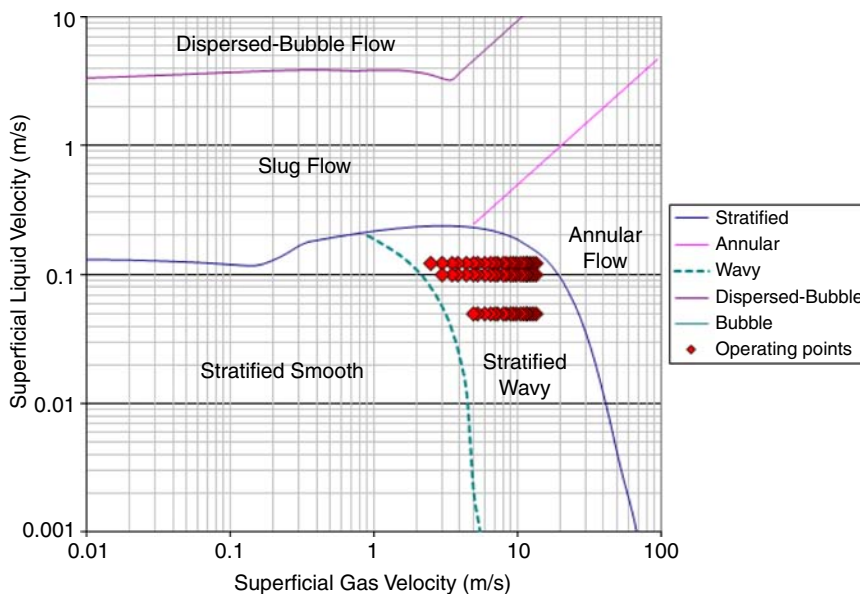

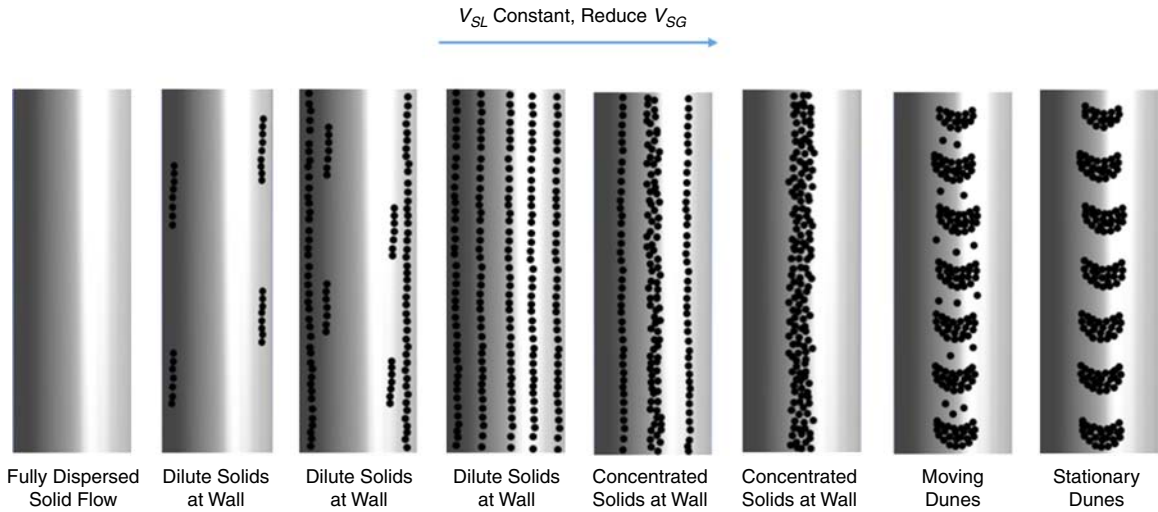Fig. 7—Taitel and Dukler (1976) flow-pattern map (Shoham 2006).

| Fully Dispersed Solid Flow | Dilute Solids at Wall | Dilute Solids at Wall | Dilute Solids at Wall | Concentrated Solids at Wall | Concentrated Solids at Wall | Moving Dunes | Stationary Dunes |

Fig. 8—Flow-regime sequences of 45–90-µm particles (bottom view).

thors hypothesize that these small particles can become trapped; however, they do not appear to affect the striations at all.

With increasing liquid holdup, the interface turbulence has less influence on the particles, and the particles have less tendency to follow counter-rotating longitudinal vortices. Therefore, because of gravity, the particles in the streaks move toward the pipe center, and a moving bed is created at the pipe bottom. The liquid velocity above the bed increases as a result of a reduction of its cross-sectional area, and a wavy profile is observed at the upper part of the bed, which moves at higher local velocities in comparison with the bottom solid-particles layer. Over time and with further reduction in gas velocity, the amplitudes of the wave profile at the top layer of solid particles grow, and they become the same size as the initial bed thickness. This phenomenon causes the concentrated solids at the wall (moving beds) that are created at the pipe bottom to disconnect and become moving dunes. Under these flow conditions, the dunes creep at the pipe bottom. Finally, at considerably low gas velocities, the particles stop moving and remain at rest at the pipe bottom, and stationary dunes are observed.

Stationary bed was not observed for this case because of the unique particle-transport mechanism (Dabirian et al. 2016). Because the particle size is very small (45–90 µm), the sand particles

on top of the bed move on the basis of the saltation mechanism (i.e., particles existing on the top of the bed are picked up and bounced to other places on the bed). A continuous saltation process leads to smaller sand particles that are collected behind larger particles that are moving at lower velocities, causing sand piles to form on top of the bed and resulting in a wavy sand-bed profile. The sand particles on top of the piles move at higher velocities relative to those in the continuous bottom-bed layer. Eventually, smaller sand particles get trapped between sand piles and start moving by either saltation or rolling mechanisms, and gaps are created between piles, which result in formation of stationary dunes.

Particle Size: 125–250 µm. Similar to the 45- to 90-µm particles at high gas velocities, the 125- to 250-µm particles are suspended in the liquid phase. Because the particles are larger, a higher gas velocity is required to keep the particles suspended in the liquid phase. With decreasing gas velocities, there are irregular motions of solid-particles streaks at the pipe, which are caused by the effect of particles on the striations. **Fig. 9** shows the flow-regime sequences for particles ranging in size from 125 to 250 µm.

At lower velocities, the solid-particles streaks are joined toward the center of the pipe, and a moving bed is observed. The moving bed is formed at wide ranges of gas velocities (whereas, with par-
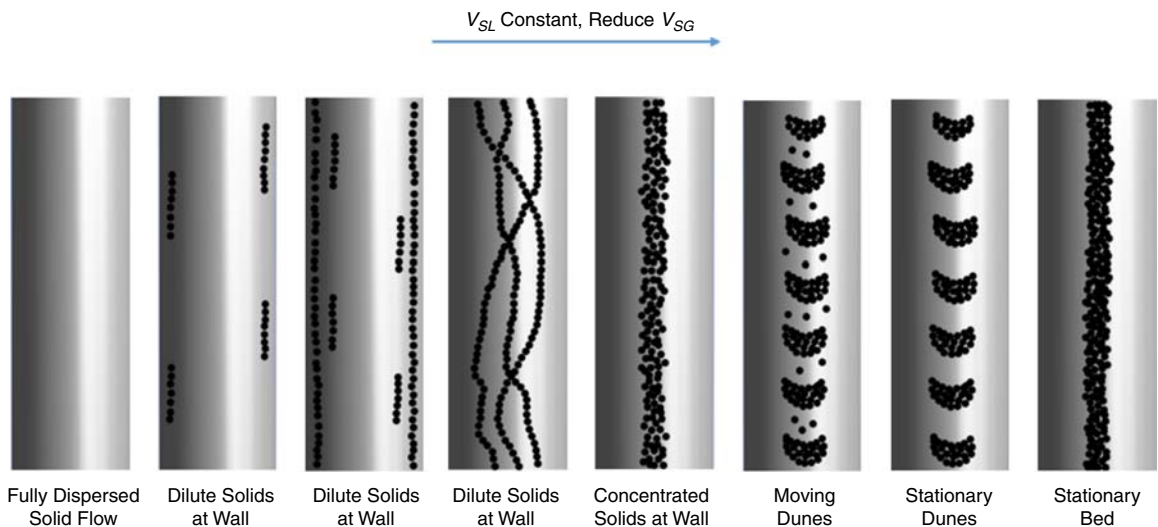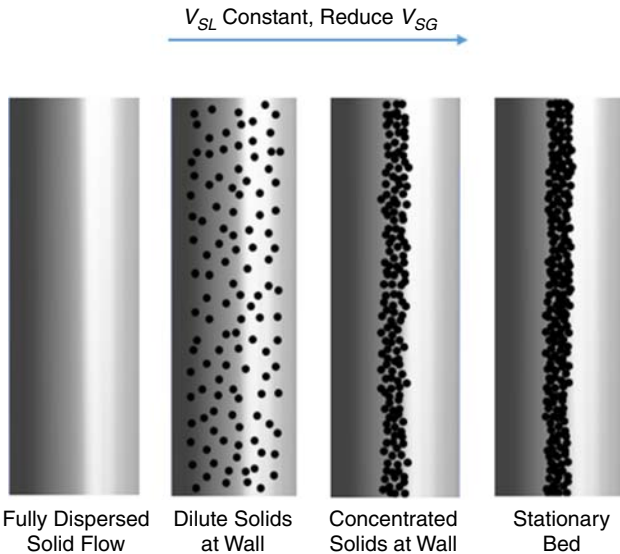
| Fully Dispersed Solid Flow | Dilute Solids at Wall | Dilute Solids at Wall | Dilute Solids at Wall | Concentrated Solids at Wall | Moving Dunes | Stationary Dunes | Stationary Bed |

Fig. 9—Flow-regime sequences of 125- to 250-µm particles (bottom view).

V_{SL} Constant, Reduce V_{SG}

| Fully Dispersed Solid Flow | Dilute Solids at Wall | Concentrated Solids at Wall | Stationary Bed |

Fig. 10—Flow-regime sequences of 425- to 600-µm particles (bottom view).

ticles ranging in size from 45 to 90 µm, the bed exists for only a narrow range of gas velocities), and it can be switched to the moving dune quickly.

Because bed thickness at concentrations less than 2,000 ppm is small, the moving bed can be turned easily into moving dunes by turbulent interface, which tends to form clusters of solid particles at the pipe bottom. However, at higher concentrations, only a wavy profile is created at the top solid-particles layer, there is a continuous bed at the bottom solid-particles layer, and no dunes are observed in the pipe. Finally, at low gas velocities, stationary dunes are observed at low solid-particles concentrations, while a stationary bed is seen at higher concentrations.

Particle Size: 425–600 µm. Because of the heaviness of the particles in this size range, they become suspended in the liquid phase only at considerably higher gas velocities. Particles undergo chaotic motions at lower velocities, and hence, they do not fall into the striations at all. At this condition, the particles prefer to roll on the

pipe, where there is lower chance of particle/particle interaction. If velocity is reduced further, increased particle interactions occur on the wall. In this situation, particles push each other instead of rolling along the pipe.

For particles ranging in size from 425 to 600 µm, no moving dunes are observed at any specific solid-particles concentrations, and particles move along the pipe bottom as a moving bed. At low gas velocities, the particles stop moving, and a stationary bed is formed. **Fig. 10** presents the flow-regime sequences for 425- to 600-µm particles.

Critical Solid-Particles-Deposition Velocity. The results for V_{SL} = 0.05, 0.1, and 0.12 m/s with the particle sizes of 45–90, 125–250, and 425–600 µm are presented, where the liquid-film velocity is defined as follows:

$$V_L = \frac{V_{SL}}{H_L}, \quad ....(3)$$

where V_{SL} is the superficial liquid velocity and H_L is the liquid holdup, which is defined as the volume fraction of the pipe that is occupied by the liquid phase.

Particle Sizes: 45–90 µm. For the small particle sizes of 45–90 µm, all solid-particles flow regimes are observed at the pipe bottom. **Figs. 11, 12, and 13** present the liquid-film velocity for 45- to 90-µm particle size over the concentration range of 100 to 10,000 ppm for V_{SL} = 0.05, 0.1, and 0.12 m/s, respectively. As can be seen, fully dispersed solid flow is observed at higher liquid-film velocities for concentrations less than 2,000 ppm, but for concentrations greater than 2,000 ppm, the liquid turbulence is not high enough to pick up all the particles. Dilute solid flow is observed in wide ranges of liquid-film velocities at three superficial liquid velocities in all concentration ranges in the form of solid-particle streaks moving parallel to each other; with increasing solid-particle concentrations, thicker solid-particle streaks are created at the pipe bottom. Concentrated solid flow forms as a moving bed for a small range of liquid-film velocities, but for all solid-particles concentrations tested, and transition to this solid-particles flow regime increases slightly with increase in concentration. For instance, the concentrated solid flow at concentrations greater than 1,000 ppm is created in a small liquid-film-velocity range of V_L = 0.55 m/s to
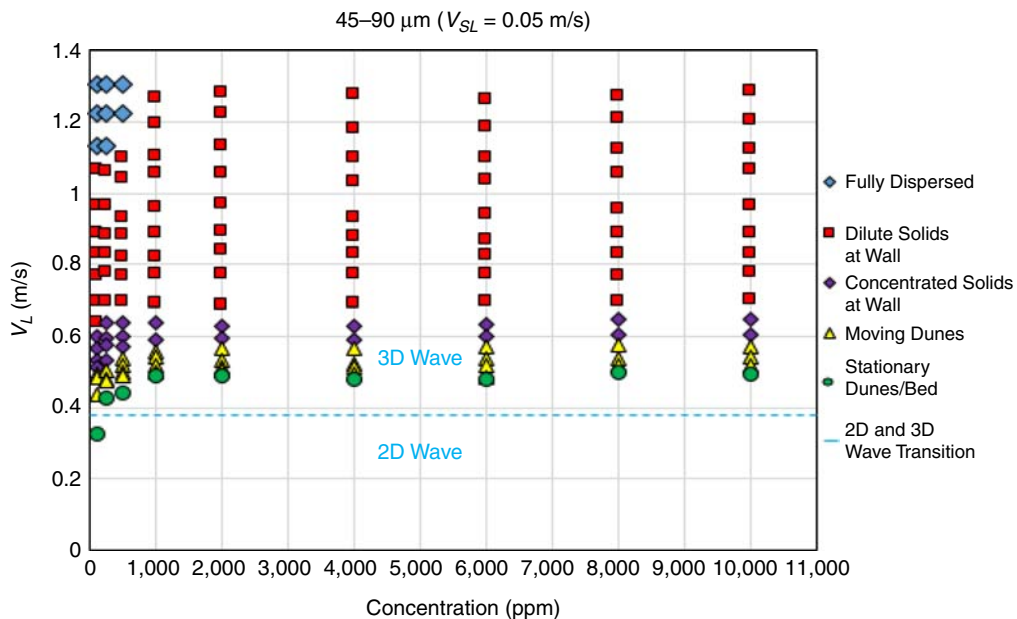
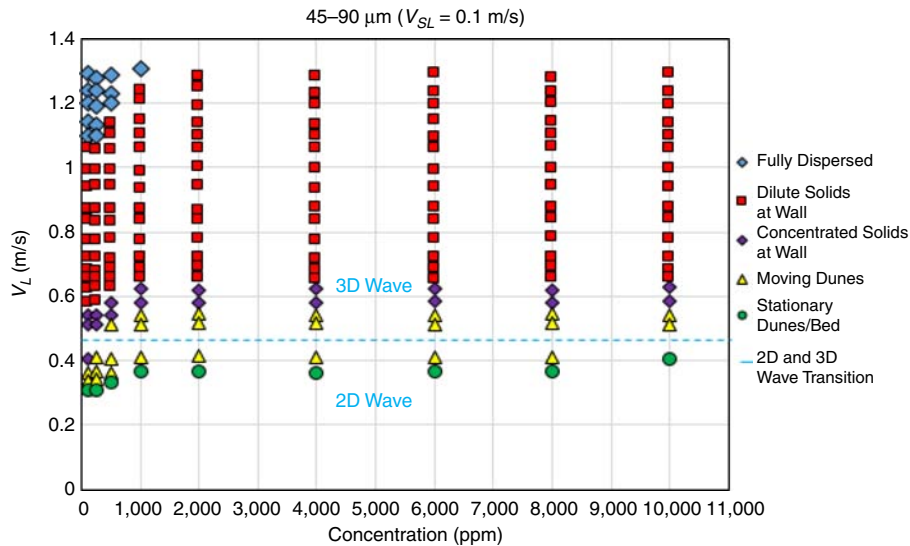**Fig. 11—Liquid-film velocity vs. concentration for V_{SL} = 0.05 m/s and particle size of 45–90 µm.**

Fig. 12—Liquid-film velocity vs. concentration for V_{SL} = 0.1 m/s and particle size of 45–90 µm.

V_L = 0.65 m/s at V_{SL} = 0.05, 0.1, and 0.12 m/s. At V_{SL} = 0.05 m/s, moving dunes are observed in the region where 3D waves occur at the gas/liquid interface, while at V_{SL} = 0.1 and 0.12 m/s, moving dunes are observed in the region where there is a transition between 2D and 3D waves at the interface. With increase in the solid-particle concentration, the size of moving dunes is increased at the pipe bottom. At considerably low superficial gas velocities (indicated by low V_L), stationary dunes are seen over all solid-particle concentrations, and no stationary bed is observed at the pipe bottom. For the particle size of 45–90 µm, the critical solid-particle-deposition velocity is defined as the transition from moving dunes to stationary dunes. As can be seen in Figs. 11, 12, and 13, the critical solid-particles-deposition velocity increases slightly with solid-particles concentration. The critical solid-particles-deposition velocities for V_{SL} = 0.1 and 0.12 m/s are almost the same, while for V_{SL} = 0.05 m/s, higher critical solid-particles-deposition velocity is required to keep particles moving continuously at the pipe bottom.

Particle Size: 125–250 µm. Similar to the 45- to 90-µm particles, all solid-particle flow regimes are observed for 125–250 µm. Fully dispersed solid flow is observed at higher liquid-film velocities for concentrations less than 1,000 ppm, and compared with the 45- to 90-µm case, the 125- to 250-µm solid particles need higher liquid velocity to suspend the solid particles completely. There are irregular motions of particles at the pipe bottom for wide ranges of liquid velocities called dilute solid flow. For this solid-particles flow regime, at specific superficial gas velocity and solid-particles concentration, more solid-particle streaks are seen at the bottom of the liquid cross-sectional area, which move irregularly at higher superficial liquid velocity as a result of an increase in the area wetted by the liquid phase at the pipe interior. **Figs. 14, 15 and 16** present the liquid-film velocity vs. solid-particle concentration for V_{SL} = 0.05, 0.1, and 0.12 m/s, respectively.

For concentrations less than 2,000 ppm, moving dunes are observed at the pipe bottom, while for concentrations greater than
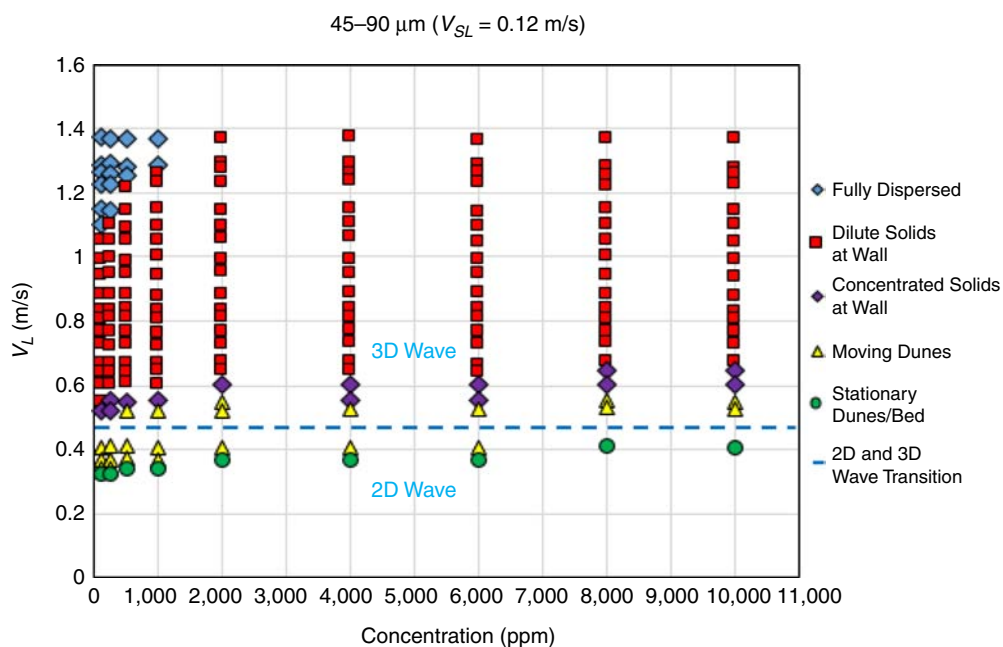

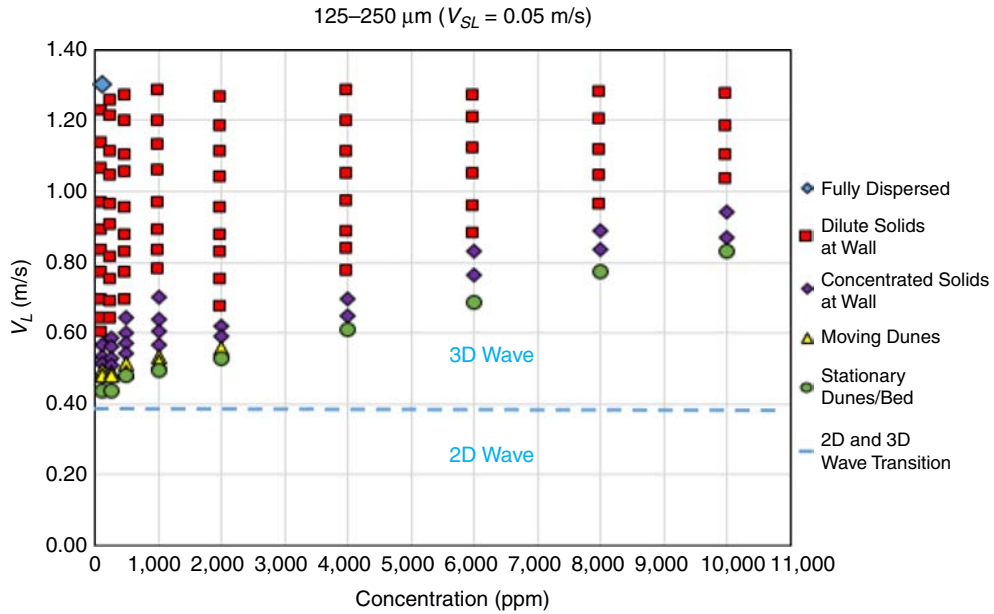**Fig. 13—Liquid-film velocity vs. concentration for V_{SL} = 0.12 m/s and particle size of 45–90 µm.**

Fig. 14—Liquid-film velocity vs. concentration for V_{SL} = 0.05 m/s and particle size of 125–250 µm.

2,000 ppm, no dunes are observed at the pipe bottom. At V_{SL} = 0.05 m/s, moving dunes are seen in the 3D wave region, while at V_{SL} = 0.1 and 0.12 m/s, the dunes are observed in the transition region for 2D and 3D waves. At concentrations less than 2,000 ppm, the critical solid-particle-deposition velocity is defined as the transition between moving dunes and stationary dunes, and it increases gradually with concentration, while for concentrations greater than 2,000 ppm, the critical solid-particle-deposition velocity is defined as the transition between concentrated flow and stationary bed, and it increases exponentially with concentration. From Figs. 14 through 16, it could be concluded that higher superficial liquid velocity needs lower critical solid-particles-deposition velocity to keep particles moving continuously at the pipe bottom.

Particle Size: 425–600 µm. To reach a fully dispersed solid flow, a higher liquid-film velocity is required as compared with other particle sizes. At V_{SL} = 0.05 m/s, no fully dispersed solid flow

is observed, even at high V_{SG} = 13.5 m/s (corresponding to V_L = 1.4 m/s), while fully dispersed solid-particles flow regime occurs at very low concentrations of less than 500 ppm for V_{SL} = 0.1 and 0.12 m/s. Chaotic motions of particles are observed as a dilute solid flow regime for a wide range of liquid-film velocities. As can be seen in **Figs. 17, 18, and 19,** no moving dunes are observed for the particle size of 425–600 µm for the entire range of solid-particles concentrations tested for V_{SL} = 0.05, 0.1, and 0.12 m/s, and the critical solid-particles-deposition velocity is defined as the transition from the concentrated solid flow to the stationary bed. Figs. 17 through 19 show that the critical solid-particles-deposition velocity increases for the entire concentration range. For V_{SL} = 0.05 m/s, the stationary bed for all solid-particles concentrations is seen in the 3D wave, while the stationary solid-particles flow regime is observed in the 2D wave for V_{SL} = 0.1 and 0.12 m/s at concentrations less than 500 ppm.
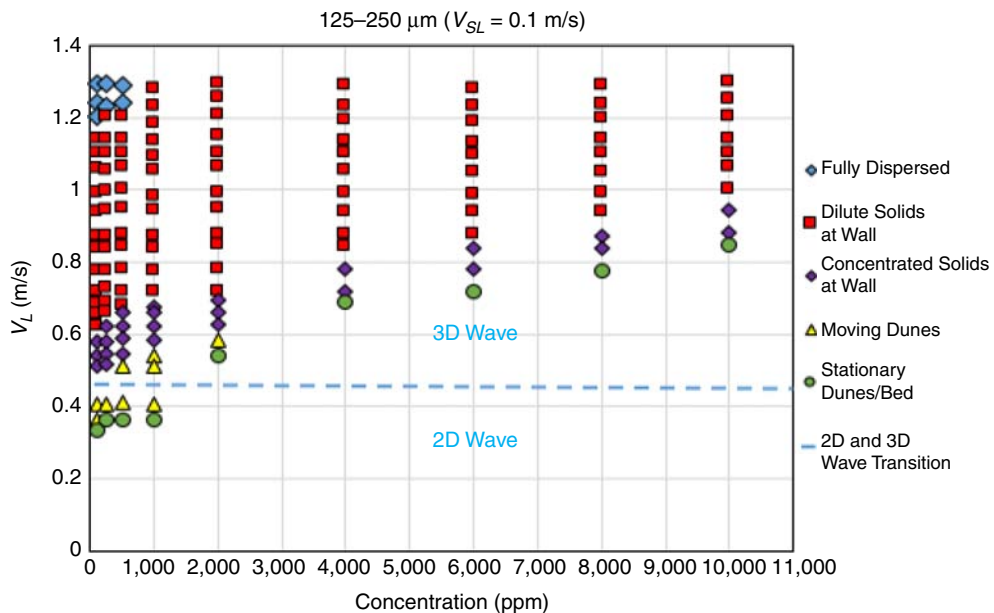

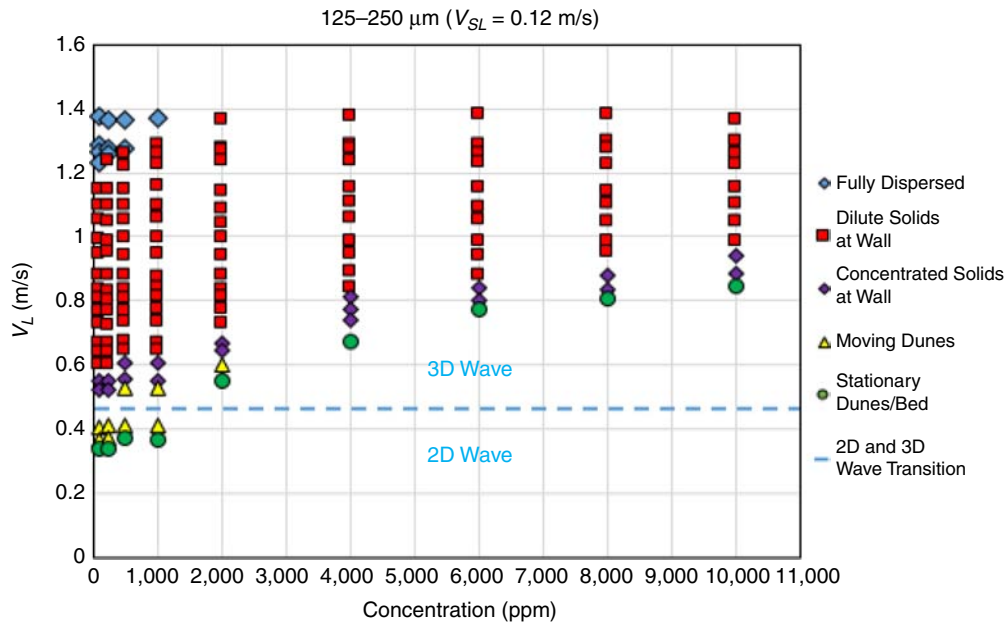Fig. 15—Liquid-film velocity vs. concentration for V_{SL} = 0.1 m/s and particle size of 125–250 µm.

125–250 μm (V_{SL} = 0.12 m/s)

Fig. 16—Liquid-film velocity vs. concentration for V_{SL} = 0.12 m/s and particle size of 125–250 μm.

Critical Solid-Particle-Deposition Comparisons. Figs. 20, 21, and 22 show the critical solid-particle-deposition velocity comparisons for particle sizes of 45–90, 125–250, and 425–600 μm for horizontal air/water/solid flow at V_{SL} = 0.05, 0.1, and 0.12 m/s, respectively. Experimental data reveal that for the particle size of 45–90 μm, the critical velocity increases slightly with concentration, while for the particle size of 125–250 (>2,000 ppm) and 425–600 μm, the velocity increases exponentially with concentration. The comparisons of critical solid-particle-deposition velocities between the particle sizes of 45–90, 125–250, and 425–600 μm show that with increase in the particle size, higher critical solid-particles-deposition velocity is required to transport all particles. Also, the experimental results show that less critical solid-particle-deposition velocity differences are seen between the particle sizes of 125–250 and 425–600 μm as compared with the particle sizes of 45–90 and 125–250 μm, which confirms that with an increase in particle size, similar trends for the critical solid-particles-deposition velocities are observed, especially at high concentrations.

The authors believe that similar trends between the 125- to 250-μm and 425- to 600-μm particles occur because of the existence of two forces—friction and drag—which have opposite effects on the critical solid-particles-deposition velocity. The 425- to 600-μm particle is heavier compared with the 125- to 250-μm particle, and, as a result, experiences larger frictional force. Hence, it requires higher critical solid-particles-deposition velocity to keep the particles moving. However, the 425- to 600-μm particle experiences a higher drag force from the surrounding liquid as a result of the larger cross-sectional area perpendicular to the fluid direction, which leads to the reduction in critical velocity needed to move the particles continuously.
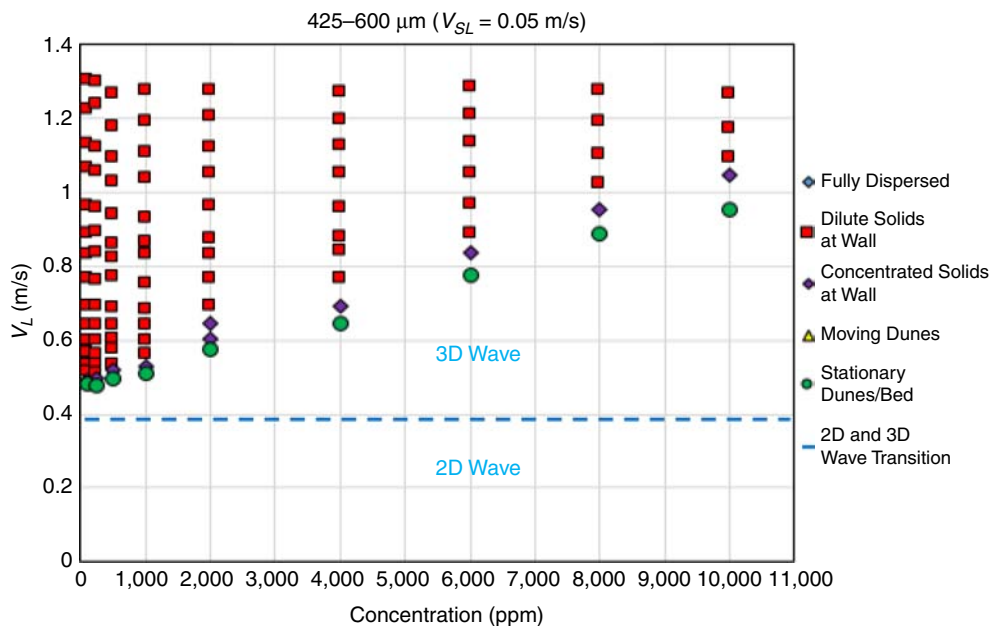

425–600 μm (V_{SL} = 0.05 m/s)

Fig. 17—Liquid-film velocity vs. concentration for V_{SL} = 0.05 m/s and particle size of 425–600 μm.

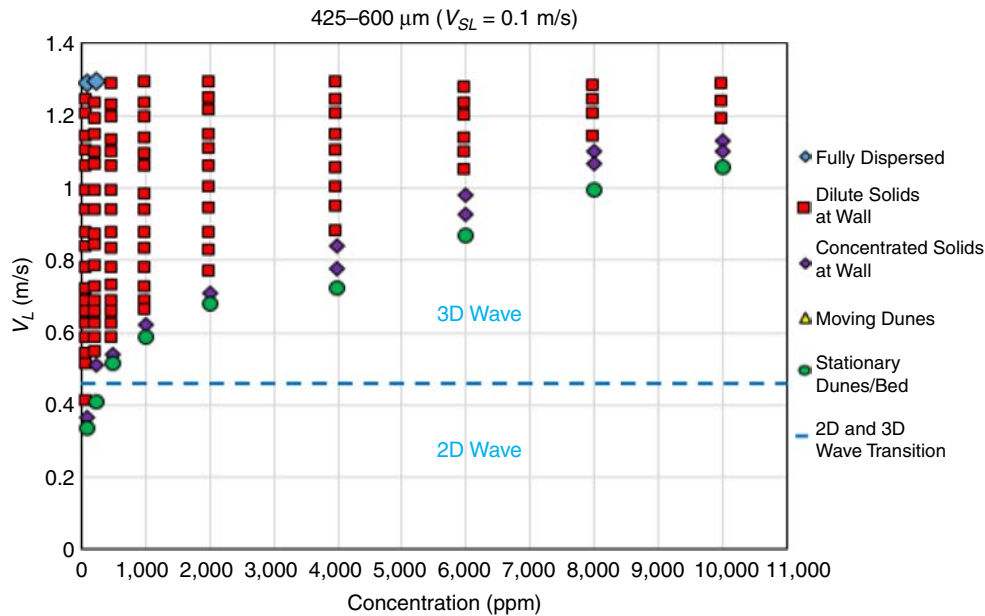**Fig. 18—Liquid-film velocity vs. concentration for V_{SL} = 0.1 m/s and particle size of 425–600 μm.**

Conclusions

Experimental studies have been conducted to study the hydraulic behavior of air/liquid/solid flow in horizontal stratified flow at solid-particle-concentration ranges of 100 to 10,000 ppm. A summary of the experimental study and main conclusions are presented as follows:

- A unique test facility is designed and constructed with a horizontal 4-in. transparent PVC pipe, which enables the measurement of superficial velocity, liquid-film velocity, liquid holdup, and pressure drop. The designed test loop uses water as liquid phase, air as gas phase, and glass beads as the solid particles. This allows determination of solid-particle flow regimes and critical solid-particle-deposition velocity.

- On the basis of this study, five solid-particle flow regimes are defined as stratified flow: fully dispersed solid flow, dilute solid flow, concentrated solid flow, moving dunes, and stationary dunes/beds.

- An ultrasonic sensor measures the liquid height at the pipe center, but quantifying holdup on the basis of the liquid height is not reliable. To calculate liquid holdup accurately, a double-circle model is applied. According to this model, the liquid holdup is calculated by measuring the liquid height at the pipe center and the pipe side.

- Flow-regime sequences for three particle sizes of 45–90, 125–250, and 425–600 μm are investigated in this study. Gas ve-
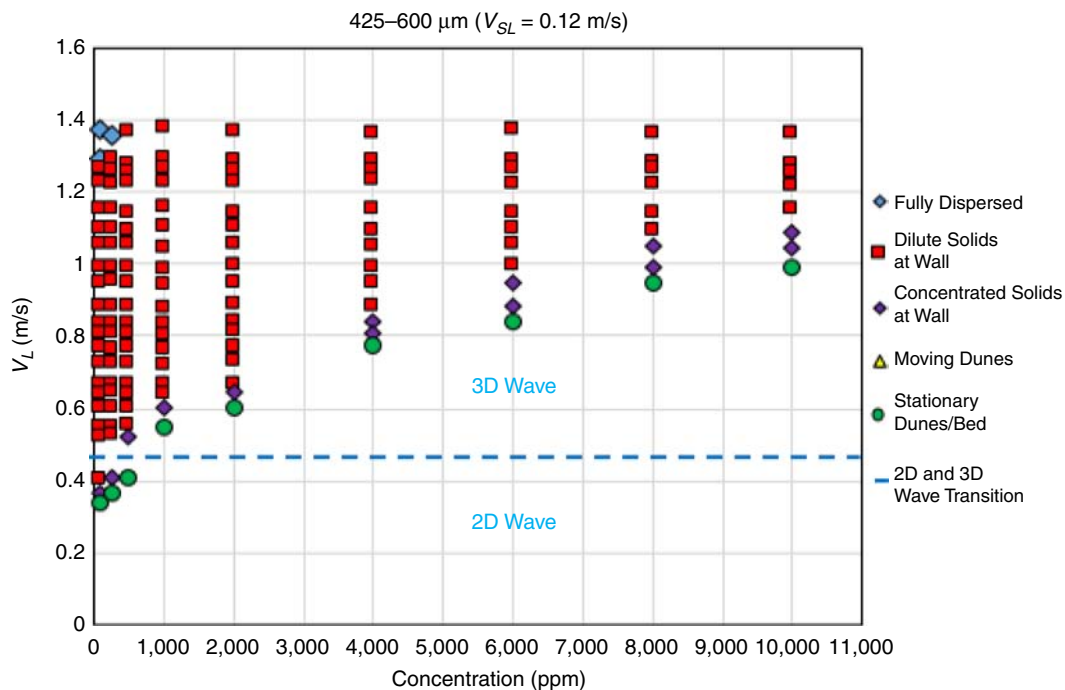

Fig. 19—Liquid-film velocity vs. concentration for V_{SL} = 0.12 m/s and particle size of 425–600 μm.

Particle-Size Comparision (V_{SL} = 0.05 m/s)

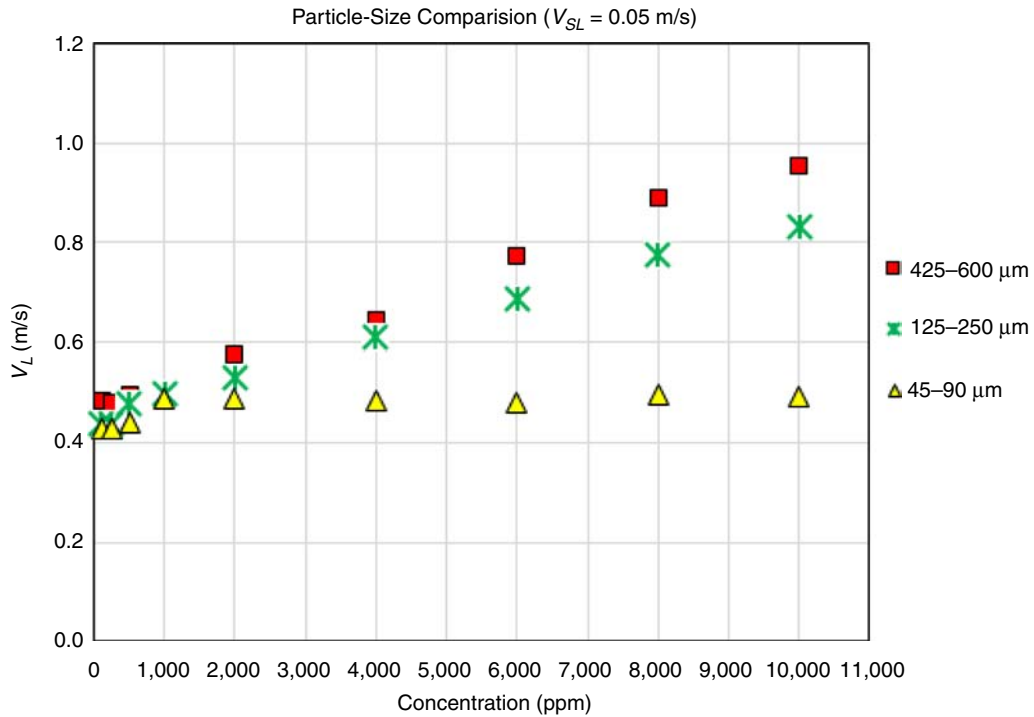**Fig. 20—Critical solid-particles-deposition velocity comparison for particle sizes of 45–90, 125–250, and 425–600 μm for horizontal air/water/solid flow at V_{SL} = 0.05 m/s.**

locity, liquid holdup, and solid-particle concentrations play important roles in the creation of different solid-particles flow-regime sequences.
• Critical solid-particle-deposition velocities show different trends with different solid-particle sizes. The experimental re-

sults reveal that when the particle sizes increase, the critical solid-particles-deposition velocity increases. Also, as the particle concentration increases, the critical solid-particles deposition velocity is fairly uniform for smaller particle sizes and increases gradually for larger particle sizes (≥ 125–250 μm).
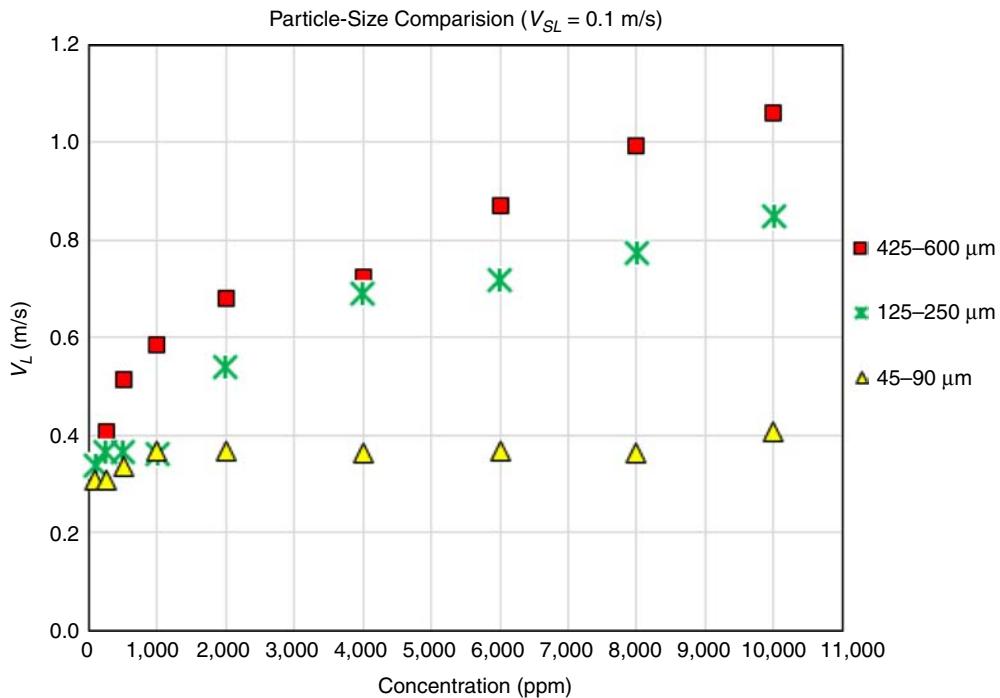
Particle-Size Comparision (V_{SL} = 0.1 m/s)

Fig. 21—Critical solid-particles-deposition velocity comparison for particle sizes of 45–90, 125–250, and 425–600 μm for horizontal air/water/solid flow at V_{SL} = 0.1 m/s.

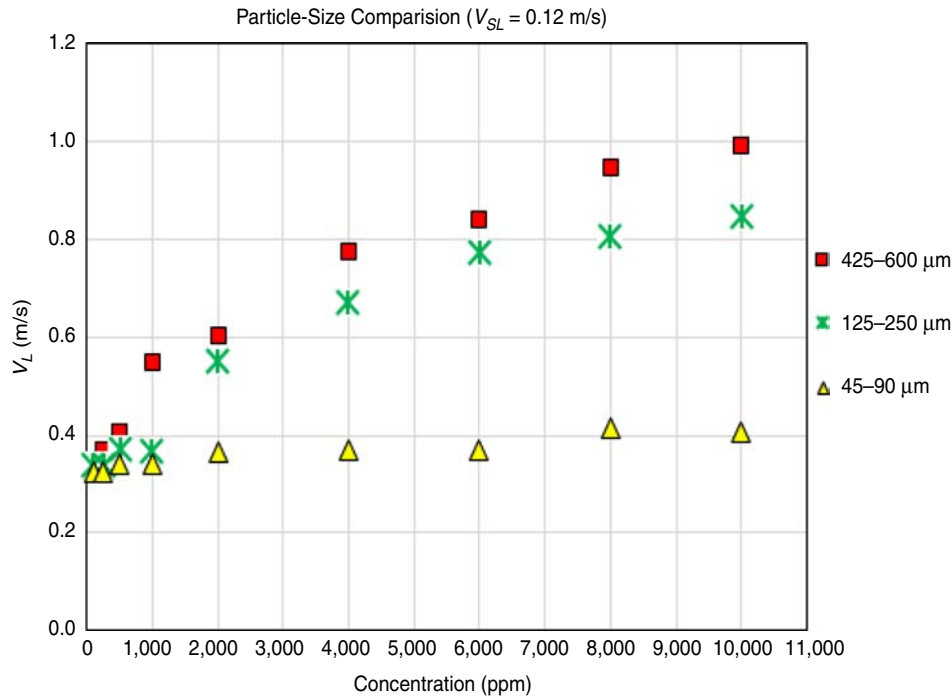**Fig. 22—Critical solid-particles-deposition velocity comparison for particle sizes of 45–90, 125–250, and 425–600 μm for horizontal air/water/solid flow at V_{SL} = 0.12 m/s.**

Nomenclature

H_L = liquid holdup
V_L = liquid-film velocity, m/s
$V_{L,C}$ = critical solid-particles-deposition velocity, m/s
V_{SG} = superficial gas velocity, m/s
V_{SL} = superficial liquid velocity, m/s
θ_0 = central angle with a flat gas/liquid interface, radians
θ_1 = central angle with a concave gas/liquid interface, radians
θ_2 = angle shown in Fig. 6, radians

Acknowledgments

References

Brauner, N., Rovinsky, J., and Maron, D. M. 1996. Determination of the Interface Curvature in Stratified Two-Phase Systems by Energy Considerations. *International Journal of Multiphase Flow* **22** (6): 1167–1185. http://dx.doi.org/10.1016/0301-9322(96)00046-8.

Dabirian, R., Mohan, R., Shoham, O. et al. 2015. Sand Transport in Stratified Flow in a Horizontal Pipeline. Presented at the SPE Annual Technical Conference and Exhibition, Houston, 28–30 September. SPE-174960-MS. http://dx.doi.org/10.2118/174960-MS.

Dabirian, R., Mohan, R., Shoham, O. et al. 2016. Sand Flow Regimes in Slightly Upward Inclined Gas-Liquid Stratified Flow. *Proc.,* ASME 2016 Fluids Engineering Division Summer Meeting, Washington, DC, 10–14 July. FEDSM2016-7729.

Doron, P. and Barnea, D. 1996. Flow Pattern Maps for Solid-Liquid Flow in Pipes. *International Journal of Multiphase Flow* **22** (2): 273–283. http://dx.doi.org/10.1016/0301-9322(95)00071-2.

Ibarra, R., Mohan, R. S., and Shoham, O. 2016. Investigation of Critical Sand-Deposition Velocity in Horizontal Gas/Liquid Stratified Flow. *SPE Prod & Oper.* SPE-168209-PA (in press; posted 15 July 2016). http://dx.doi.org/10.2118/168209-PA.

Nguyen, H., Wang, S., Mohan, R. S. et al. 2014. Experimental Investigations of Droplet Deposition and Coalescence in Curved Pipes. *J. Energy Resour. Technol.* **136** (2): 022902, 6 pages. JERT-13-1197. http://dx.doi.org/10.1115/1.4026916.

Salama, M. M. 1999. Sand Production Management. *J. Energy Resour. Technol.* **122** (1): 29–33. http://dx.doi.org/10.1115/1.483158.

Shamlou, P. A. 1987. Hydraulic Transport of Particulate Solids. *Chem. Eng. Comm.* **62** (1–6): 233–249. http://dx.doi.org/10.1080/00986448708912062.

Shoham, O. 2006. *Mechanistic Modeling of Gas-Liquid Two-Phase Flow in Pipes*. Richardson, Texas: Society of Petroleum Engineers.

Shook, C. A., and Roco, M. C. 1991. *Slurry Flow: Principles and Practice*. Boston, Massachusetts: Butterworth-Heinemann Series in Chemical Engineering, Elsevier.

Taitel, Y. and Dukler, A. E. 1976. A Model for Predicting Flow Regime Transitions in Horizontal and Near-Horizontal Gas-Liquid Flow. *AIChE Journal* **22** (1): 47–55. http://dx.doi.org/10.1002/aic.690220105.

Wilson, K. C. 1976. A Unified Physically-Based Analysis of Solid-Liquid Pipeline Flow. *Proc.,* 4th International Conference on the Hydraulic Transport of Solids in Pipes, Banff, Alberta, Canada, Paper A1, 1–16.

Wood, D. J. 1979. Pressure Gradient Requirements for Re-Establishment of Slurry Flow. *Proc.,* 6th International Conference on the Hydraulic Transport of Solids in Pipes, Canterbury, England, Paper D4, 217–228.

Yongqian, F. 2005. *An Investigation of Low Liquid Loading Gas-Liquid Stratified Flow in near-Horizontal Pipes*. PhD dissertation, The University of Tulsa.

Ramin Dabirian holds a PhD degree in mechanical engineering from The University of Tulsa. He joined The University of Tulsa as a research assistant in the TUSTP group in pursuit of an MS degree in petroleum engineering. Dabirian's research interests are multiphase-flow modeling in pipelines and multiphase separation and transportation. He holds a BS degree in petroleum engineering from the Petroleum University of Technology, Iran. Dabirian is a member of SPE.

Ram S. Mohan is a professor of mechanical engineering at The University of Tulsa and a fellow of the American Society of Mechanical Engineers.

He teaches and conducts research in the areas of multiphase flow, oil/water dispersion, instrumentation and measurements, control systems, compact separators, computer-aided design, and manufacturing processes. Mohan currently serves as the codirector of TUSTP, supported by several oil companies. He also directs several projects supported by the Chevron Tulsa University Center of Research Excellence. Mohan has authored or coauthored more than 75 refereed publications in the areas of his research, holds four patents/invention disclosures, and has received several best-paper awards. He holds a BSc degree in mechanical engineering from the University of Kerala, India, and MS and PhD degrees in mechanical engineering from the University of Kentucky. Mohan is a member of SPE.

Ovadia Shoham is the F. M. Stevenson Distinguished Presidential Chair Professor of Petroleum Engineering at The University of Tulsa. Since 1994, he has directed TUSTP, conducting research on compact separators and several projects supported by industry. Shoham has authored or coauthored more than 90 publications in the areas of multiphase flow, multiphase separation, and production operations and holds four patents/invention disclosures. He holds BS and MS degrees in chemical engineering from the Technion in Israel and the University of Houston, respectively, and a PhD degree in mechanical engineering from Tel Aviv University. Shoham has published a widely referenced SPE book, *Mechanistic Modeling of Gas-Liquid Flow*. He is the recipient of the 2003 SPE International Production and Operations Award and has received several best-paper awards. Shoham is a member of SPE.

Gene Kouba is retired from Chevron, where he was a research consultant for their Energy Technology Company. His primary research interests include issues in multiphase-flow transport and separation. Kouba has authored or coauthored 88 technical papers and holds eight patents. He holds a PhD degree in petroleum engineering from The University of Tulsa. Kouba was the recipient of the 2014 SPE Projects, Facilities, and Construction Award.